Fermi National Accelerator Laboratory

FERMILAB-Conf-98/314-E
CDF

Dijet Measurements at CDF and D0

J. Lamoureux
For the CDF Collaboration

Brandeis University

Fermi National Accelerator Laboratory
P.O. Box 500, Batavia, Illinois 60510

October 1998

Published Proceedings of the *29th International Conference on High Energy Physics, ICHEP98*, Vancouver, B.C., Canada, July 23-29, 1998

Operated by Universities Research Association Inc. under Contract No. DE-AC02-76CH03000 with the United States Department of Energy

DIJET MEASUREMENTS AT CDF AND D0

JODI LAMOUREUX
Brandeis University
for the CDF Collaboration
Fermi National Accelerator Laboratory, MS 318
P.O. Box 500
Batavia, IL, 60510

A preliminary measurement of the differential dijet cross section obtained from $p\bar{p}$ colisions at $\sqrt{s} = 1.8$ TeV by the CDF collaboration is presented. The D0 and CDF dijet mass distributions are also presented. Measured distributions are compared to NLO QCD predictions. The effect of changing the renormalization scale and the choice of the parton density functions on the predicted cross sections is shown. Finally, limits for new particle production are presented based on the dijet mass and angular distributions.

1 Introduction

Jet distributions at high-energy colliders can be used to test quantum chromodynamic (QCD) predictions and search for new particle production. In addition, since the observed jet production rates at proton-antiproton colliders are the result of convoluting the QCD cross sections with the parton densities in the proton, the parton-distribution functions (PDFs) can also be extracted.

The inclusive jet measurements presented at this conference show that in general the next-to-leading order (NLO) QCD prediction [1] describes the jet spectrum as its production cross section falls nine orders of magnitude [2]. A detailed comparison of the CDF data indicates an excess of events at high E_T when compared to the QCD predictions with standard PDFs [3]. This excess has generated a great deal of theoretical interest [4] including several new sets of PDFs which include the CDF measurement in determining the PDFs [5]. In this paper, we present the dijet differential and mass distributions and compare them to NLO QCD predictions.

One possible explanation for the increased jet production at high E_T is that there is a new particle, never before detected, which makes an additional contribution to the cross section. Since the jet spectra extend to higher E_T than any other measured spectra at the Tevatron, we hope that someday it may show us the first evidence of quark substructure (compositeness [6]). In order to test the new particle hypothesis, we measure the dijet angular distributions which are relatively insensitive to variations in the PDFs. Limits on quark compositeness and coloron production are presented in section 4.

2 The Differential Dijet Cross Section

Preliminary results for the differential dijet cross section, $d\sigma/(dE_T d\eta_1 d\eta_2)$ are presented by the CDF collaboration for the 1994-1995 Fermilab Tevatron Collider run. This distribution is made by plotting the E_T spectrum of a *trigger* jet ($E_T > 40$ GeV, $0.1 < |\eta_1| < 0.7$) for four different bins in *probe* jet pseudorapidity. The *probe* jet is defined as any jet with $E_T > 10$ GeV. The four pseudorapidity bins are: $0.1 < |\eta_2| < 0.7$, $0.7 < |\eta_2| < 1.4$, $1.4 < |\eta_2| < 2.1$ and $2.1 < |\eta_2| < 3.0$. In all cases, the spectrum plotted is that of the *trigger* jet. In the case that the *probe* jet also satisfies the *trigger* jet selection requirements, both combinations contribute to the distribution.

Figure 1 shows the measured spectrum for the four pseudorapidity bins. The measured energies are corrected for detector resolution and smearing using the same procedure used in the measurement of the inclusive jet cross section [3]. The results are compared to the NLO QCD calculation of JETRAD [7] using several different PDFs [5]. In general, agreement is seen over six orders of magnitude.

A detailed comparison is shown in figure 2. Here the relative difference from the theoretical prediction (JE-

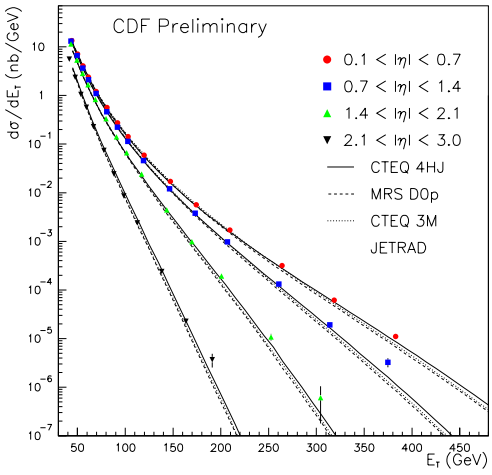

Figure 1: The preliminary measurement of the differential dijet cross section. The results are compared to the predictions of JETRAD using several different PDFs.

TRAD, Rsep=1.3, $\mu = 0.5E_T^{max}$, CTEQ 4M) is shown. For comparison, the relative difference between the theory using CTEQ 4HJ or MRST and the default theory are shown. In all four plots, the data rise at $E_T > 200$ GeV above the CTEQ 4M curve. The curvature of CTEQ 4HJ appears to be in better agreement. The MRST curve has a low E_T shape which may be hard to accomodate. The systematic uncertainty ranges from about 20-40% and can account for the normalization offsets. We note that the systematic uncertainty between the four distributions is correlated and that the character of the comparison in the high pseudorapidity bin appears to be somewhat different than in the other bins. One possible explanation is that the $O(\alpha_s^3)$ QCD predictions are not adequate to describe the high η bin which is composed of four or more jet events $> 25\%$ of the time, A full analysis of the comparison has not been done yet, and conclusions about the agreement with theory are preliminary.

The E_T and pseudorapidities of the leading jets are related to the momentum fraction, x, of the partons involved in the interaction. At leading order the relation is

$$x_1 = \frac{E_T}{\sqrt{s}}(e^{\eta_1} + e^{\eta_2}); \quad x_2 = \frac{E_T}{\sqrt{s}}(e^{-\eta_1} + e^{-\eta_2}). \qquad (1)$$

For fixed E_T and η_1, different momentum fractions can be selected by requiring that the *probe* jet lie in different

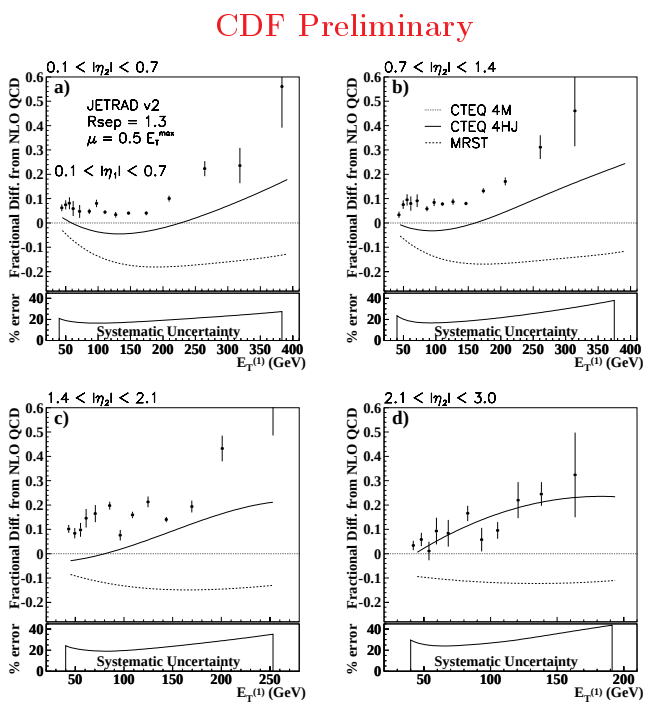

Figure 2: The fractional difference from NLO QCD for the differential dijet cross section. The four distributions in figure 1 are plotted separately here.

η intervals. We define $x_{\max}$ as the maximum of x_1 and x_2. For a two body process one intuitive choice for the QCD scale of the interaction is

$$Q^2 \sim -\hat{t} = 2E_T^2 \cosh^2\eta^*(1 - \tanh\eta^*) \qquad (2)$$

The data, converted from (E_T, η_2) bins to $(x_{\max}, \hat{t})$ bins, are shown in Figure 3 with statistical errors only. The data span a region in x and Q^2. We plan to use this two dimentional space to constrain the PDFs and α_s simultaneously.

3 The Dijet Invariant Mass Distribution

Both CDF and D0 have measured the dijet mass cross section, $\Delta d\sigma^2/\Delta M_{jj} d\eta_1 d\eta_2$, as a function of the dijet mass. The new spectrum from D0 [8], shown in figure 4 is based on 92 pb^{-1}. The mass is constructed from two jets $|\eta_{1,2}| < 1.0$.

$$M_{jj} = 2E_T^{(1)} E_T^{(2)}(cosh(\Delta\eta) - cos(\Delta\phi)) \qquad (3)$$

Masses above 200 GeV are included in the distribution. The NLO QCD prediction using JETRAD with CTEQ3M [9] and $\mu = 0.5E_T^{max}$ is shown for comparison. The fractional difference from theory is presented in the lower plot. The dijet mass distribution is observed to be insensitive to changes in renormalization scale, μ, and

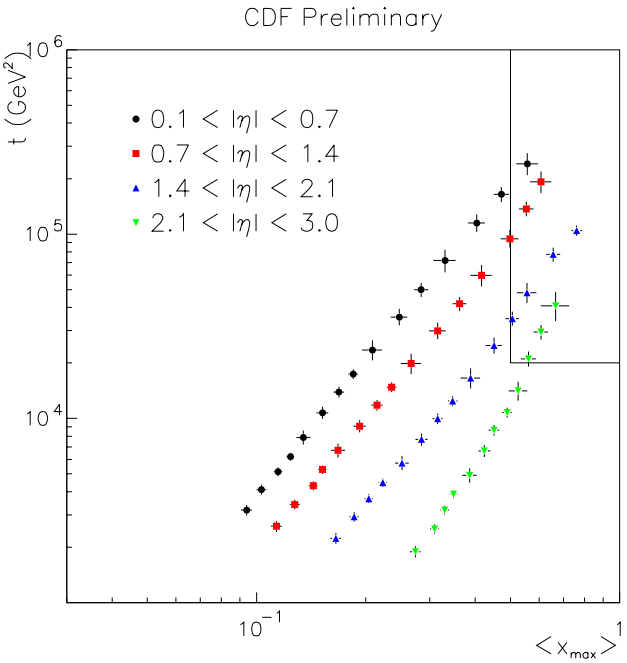

Figure 3: The $x_{\max}$ and $\hat{t}$ region probed by the differential dijet cross section measurements. Uncertainties are statistical only.

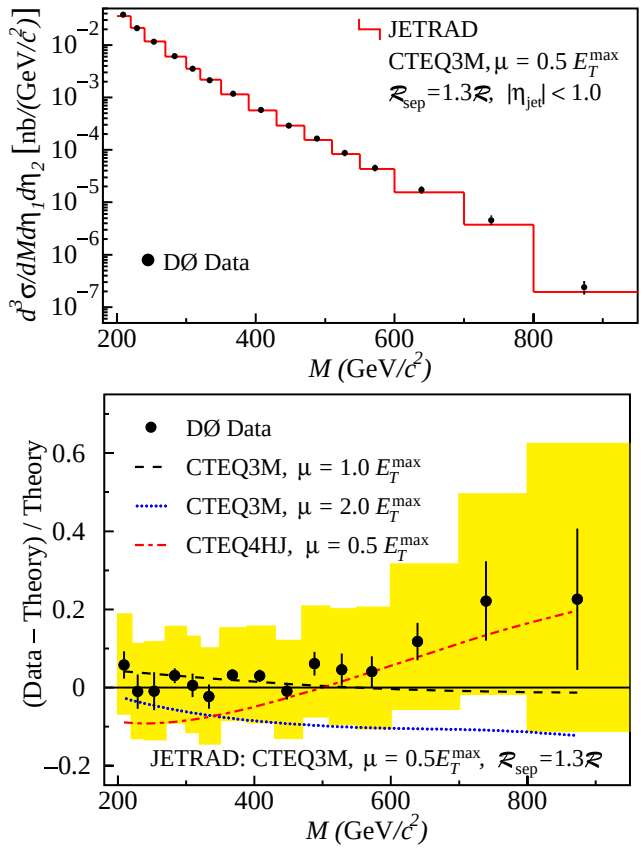

Figure 4: Dijet mass spectrum from D0 compared to NLO QCD calculated using JETRAD with CTEQ3M and $\mu = 0.5E_T^{max}$. The lower plot is the fractional difference from NLO QCD.

the PDFs. The conclusion that the data and theory are in good agreement is supported by the χ^2 analysis presented in table 1.

A comparison of the CDF and D0 results is shown in figure 5. The CDF measurement uses jets with $|\eta_{1,2}| < 2.5$ and includes the mass of each jet in the dijet mass calculation.

$$M_{jj} = \sqrt{(E_1 + E_2)^2 - (\vec{p}_1 + \vec{p}_2)^2}, \qquad (4)$$

PDF	renorm scale	χ^2 (15 DOF)	Prob(χ^2)
CTEQ3M	$0.25E_T^{max}$	12.2	0.66
CTEQ3M	$0.50E_T^{max}$	5.0	0.99
CTEQ3M	$0.75E_T^{max}$	5.3	0.99
CTEQ3M	$1.00E_T^{max}$	5.4	0.99
CTEQ3M	$2.00E_T^{max}$	4.2	1.00
CTEQ4M	$0.50E_T^{max}$	4.9	0.99
CTEQ4HJ	$0.50E_T^{max}$	5.0	0.99
MRS(A´)	$0.50E_T^{max}$	6.3	0.97

Table 1: χ^2 comparison of the D0 dijet mass data to theory.

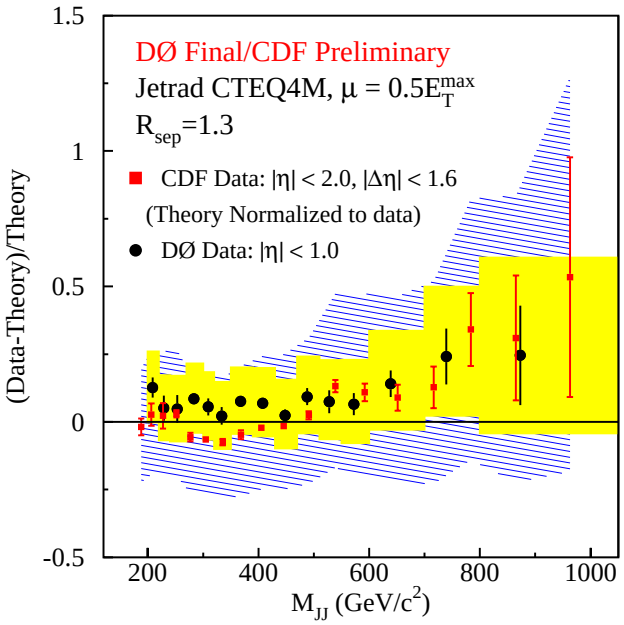

Figure 5: Comparison of the dijet mass distributions from CDF and D0 with theory predictions using JETRAD with the CTEQ4M PDF.

Since the two measurements differ somewhat, the fractional difference from NLO QCD is shown for both. The data from the two experiments is in good agreement, and also with theoretical predictions.

D0 has also measured the cross section separately in the central ($|\eta_{1,2}| < 0.5$) and forward ($0.5 < |\eta_{1,2}| < 1.0$) regions. The distributions are compared to NLO QCD in figure 6. Again good agreement is observed between the measured spectrum and the theoretical prediction.

4 Limits on New Phenomena

One possible explanation for the increased jet production at high E_T is that there is a new particle never before detected which makes an additional contribution to the cross section. Since the jet spectra extend to higher E_T than any other measured spectra at the Tevatron, we hope that someday it may show us the first evidence of quark substructure (compositeness). When the uncertainty on the gluon distribution is resolved, we can use the jet spectra directly to search for new physical phenomena. Until then, we resort to other distributions which are less sensitive to the PDFs.

D0 takes the ratio of the forward and central dijet mass spectra presented in figure 6 to search for compositeness. The ratio is shown in figure 7. Theoretical predictions are included showing increases in jet production for compositeness scales of 1.5 to 3.0 TeV. No visible increased production is observed in the data. 95% con-

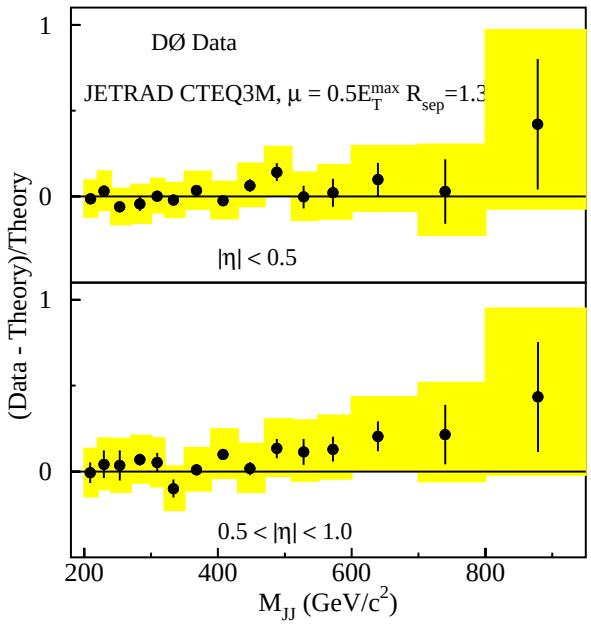

Figure 6: The preliminary D0 dijet mass distributions for central ($|\eta| < 0.5$) and forward ($0.5 < |\eta| < 1.0$) jets compared with the QCD calculation.

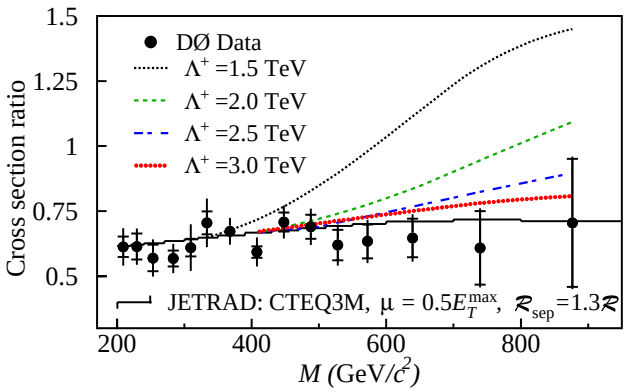

Figure 7: The ratio of the central and forward dijet mass distributions is sensitive to new particle production. Quark substructure would enhance this distribution at high mass.

fidence level limits on the contact interaction scale are listed in table 2.

Measurement of the scattering angle between the dijet and proton beam, in the center-of-mass system provides a fundamental test of QCD and is a sensitive probe of new physics. The dijet angular distribution is defined as:

$$\chi \equiv \hat{u}/\hat{t} = \frac{(1+\cos\theta^*)}{(1-\cos\theta^*)} \simeq e^{|\eta_1 - \eta_2|} \qquad (5)$$

where θ^* is the center-of-mass scattering angle. The angular distribuion is fairly insensitive to the PDFs. Two dominant sources of systematic error arise from multiple interactions and the energy scale dependence on η. As shown in figure 8, a contact interaction term changes the

D0 ratio of central/forward dijet mass:
$\Lambda^+ \geq 2.7$ TeV, $\Lambda^- \geq 2.4$ TeV.
CDF angular distribution:
$\Lambda^+ \geq 1.8$ TeV, $\Lambda^- \geq 1.6$ TeV,
$\Lambda^+_{ud} \geq 1.6$ TeV, $\Lambda^-_{ud} \geq 1.4$ TeV.
D0 angular distribution:
$\Lambda^+ \geq 2.1$ TeV, $\Lambda^- \geq 2.2$ TeV,
$\Lambda^+_{ud} \geq 1.9$ TeV, $\Lambda^-_{ud} \geq 2.0$ TeV.
D0 angular distribution:
$M_c/cot\theta \geq 759$ GeV/c^2.

Table 2: 95% confidence limits for new particle produciton based on measured dijet mass and angular distributions. Compositeness limits are expressed in terms of Λ. The coloron limit is expressed in terms of $M_c/cot\theta$.

shape of the expected distribution. The D0 data appear to be in good agreement with NLO QCD predictions [10]. A similar analysis at CDF shows the same effect [11]. 95% confidence level limits on the contact interaction scale from these analyses are listed in table 2.

Finally, using the same measured distribution as in figure 8, D0 sets limits on a universal coloron [12]. The new model proposes an octet of heavy coloron bosons in addition to ordinary massless gluons. It includes a coloron-exchange scale, M_c, and an angular term, $cot\theta$, which depends on the ratio of the gauge couplings of the regular gluons and the new gluons. The effect on the angular distribution of including a coloron is shown in figure 9. Data exclude a flavor universal coloron[13] with $M_c/cot\theta < 759$ GeV/c^2.

5 Conclusions

The differential dijet cross section can be used as an input to global QCD fits. The data span a region in x and Q^2 which we plan to exploit to constrain the PDFs and α_s simultaneously. We have seen that the data rise at high E_T above the theory predictions of CTEQ 4M and MRST, but that a modified PDF, CTEQ 4HJ, appears to reproduce the shape of the data. Conclusions about the agreement, however, are preliminary at this time, awaiting a full analysis of the comparison.

The dijet mass spectrum is observed to be in agreement with QCD predictions. The shape of the data from CDF and D0 are consistent. Within experimental uncertainties the mass distribution is insensitive to changes in renormalization scale and PDFs.

Finally we conclude that there is no evidence that the increased jet production is the result of new particle interactions. Limits on new phenomena are summarized in table 2.

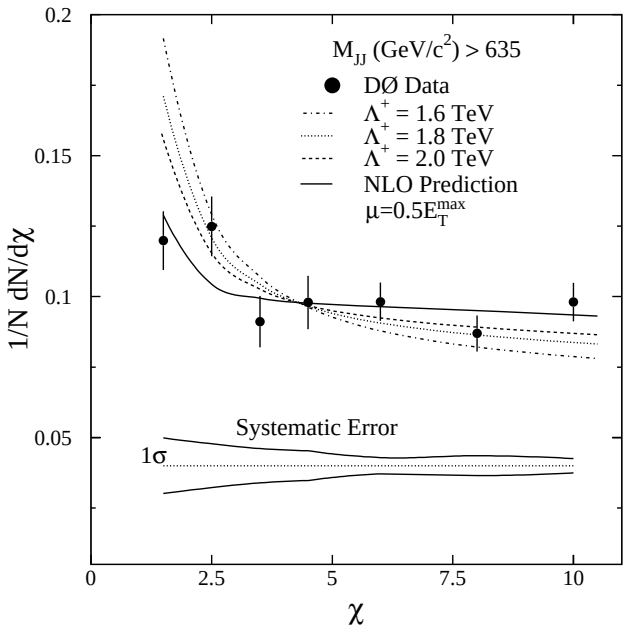

Figure 8: D0 dijet angular distribution compared to theory predictions including a contact interaction scale, Λ.

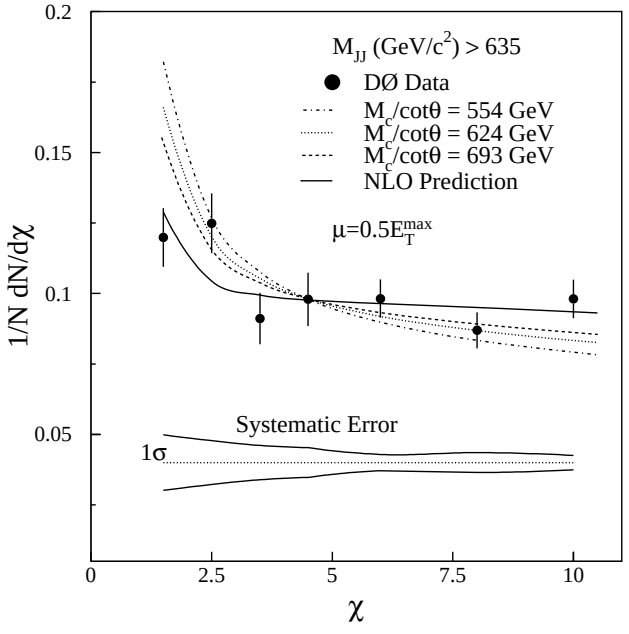

Figure 9: D0 dijet angular distribution compared to theory predictions including colorons.

Acknowledgments

We thank the staffs at Fermilab and the collaborating institutions for their contributions to this work, and acknowledge support from the Department of Energy and the National Science Foundation (U.S.A.), Commissariat à L'Energie Atomique (France), State Committee for Science and Technology and Ministry for Atomic Energy (Russia), CNPq (Brazil), Departments of Atomic Energy and Science and Education (India), Colciencias (Columbia), CONACyT (Mexico), Ministry of Education and KOSEF (Korea), and CONICET and UBACyT (Argentina).

References

1. S. Ellis *et al.*, *Phys. Rev. Lett.* **64**, 2121 (1990); W.T.Giele et al., *Nucl. Phys.* B **403**, 633 (1993).
2. G. Blazey, Proceedings, this conference.
3. F. Abe *et al.*, CDF Collab., *Phys. Rev. Lett.* **77**, 438 (1996).
4. S.Catani *et al.*, hep-ph/9604351; M.Klasen and G. Kramer, hep-ph/9605210; W.T. Giele *et al.*, *Phys. Rev.* D **53**, 120 (1996).
5. J.Huston *et al.*, CTEQ Collab., *Phys. Rev. Lett.* **77**, 444 (1996); H.L. Lai *et al.*, CTEQ Collab., *Phys. Rev.* D **55**, 1280 (1997); A.D. Martin, R.G. Roberts, W.J. Stirling and R.S. Thorne, Eur.Phys.J.C4:463,1998.
6. E. Eichten, K. Lane and M.E. Peskin, *Phys. Rev. Lett.* **50**, 811 (1983); E. Eichten, I. Hinchcliffe, K. Lane and C. Quigg, *Rev. Mod. Phys.* **56** 579(1984). addendum - ibid. **58** 1065(1986).
7. W.T. Giele, E.W.N. Glover and D.A. Kosower, *Phys. Rev. Lett.* **73**, 2019 (1994).
8. B. Abbott *et al.*, D0 Collab., FERMILAB-PUB-98-220-E, hep-ex/9807014.
9. H.L. Lai *et al.*, CTEQ Collab., *Phys. Rev.* D **51**, 4763 (1995).
10. B. Abbott *et al.*, D0 Collab., *Phys. Rev. Lett.* **80**, 666 (1998).
11. F. Abe *et al.*, CDF Collab., *Phys. Rev. Lett.* **77**, 5336 (1996); erratum - ibid. *Phys. Rev. Lett.* **78**, 4307 (1997).
12. R.S. Chivukula, A. Cohen and E.H. Simmons, *Phys. Lett.* B **380**, 92 (1996);
13. B. Abbott *et al.*, D0 Collab., FERMILAB-Conf-98/279-E, hep-ex/9809009.